

# Investigation of Mechanical Properties of Grade 23a and 080M46 Steel Specimens by Temperature Change and Heat Treatment Methods

Mohamad Danish Anis<sup>1</sup>

<sup>1</sup>School of Mechanical, Aerospace & Civil Engineering, University of Manchester, United Kingdom, danishanis10@hotmail.com

## ABSTRACT

The aim of this research paper is to study the effects of temperature change and heat treatment on the mechanical properties of stainless steel specimens by carrying out two laboratory experiments-destructive impact testing and simple tensile testing.. First, the Charpy Test was used on various Grade 23a steel test samples at different temperatures. The results of tensile testing were used to plot the conventional force vs. displacement graph for each sample and obtain the Ultimate Tensile Strength (UTS), elongation and yield stresses. The results are compared with the theoretical value and the uncertainties are stated and reasoned. The Charpy Test results were used to determine what temperature would Grade 23a steel function best at and the consequences of the application of Grade 23a to cryogenic conditions. The results of heat treatment of 080M46 steel, on the other hand, established how quenching & tempering mechanisms enhance steel toughness.

**Key words :** Charpy Test, CCT Diagrams , DBTT, Material Phases, Quenching & Tempering..

## INTRODUCTION

Iron-based alloys like steel feature as the most prominently used metallic alloys in the world of engineering today (Lo et al., 2009). The abundance of iron in the earth's crust and the ease of extraction from its ores contribute to iron being relatively inexpensive as compared to its contemporary metals. Owing to their properties and versatility, steels are arguably the most important class of engineering and construction materials in the world (Baddoo, 2008). There are many varieties of steels that go into production for specific

uses. These various types of steels differ from each other only in their carbon concentration and the presence of other alloying elements. The laboratory experiments carried out for this research investigated the changes that are brought about in mechanical properties of structural steels and medium-carbon steels. Both structural and medium-carbon steels have less than 0.5 wt. % carbon and relatively low levels of other alloying elements. Heat treatment and impact testing procedures have been the conventional laboratory methods of achieving a diverse range of material properties in iron-based alloys, steels in particular (Khaleghi et. al., 1985). The behavior of mechanical properties of different structural steel grades should be well known to understand the behavior of steel and composite structures.

## EXPERIMENTAL WORK – CHARPY IMPACT TEST

### Impact Testing Material

In this part of the laboratory experiment, research was conducted on Grade 23a steel specimens, which is equivalent to S275 or European Standard EN10025 (Callister, 2009). Figure 1 depicts a Grade 23a Structural Steel laboratory specimen used at The University of Manchester. Grade 23a stainless steel has been chosen due to its strong austenitic properties with carbon content close to 0.25 wt. %. The aim was to assess the toughness of this steel as a function of temperature. In order to carry out charpy impact tests on specimens at lower temperatures, it was necessary to immerse the specimens in liquid nitrogen and to monitor the warming of these specimens using temperature probe and a stop watch. This was done until the desired test temperature was achieved.



**Figure 1:** Grade 23a Stainless Steel Specimen used for Charpy Impact Testing (Francis, 2014).

**Ductile to Brittle Transitions in Steels – Research Background**

Charpy impact testing was conducted on Grade 23a stainless steel specimens in order to obtain a schematic representation of its DBTT. The reason being an fcc lattice having 12 closed-packed slip directions that allow molecular dislocations to glide under shear stress, thus providing ductile behavior (Gavriljuk, 2007). Due to bcc lattice exhibiting low ductility levels, they are known to undergo a ductile-to-brittle transition and have a DBT temperature (DBTT) (Pandiyan, 2008). This means that the toughness or the energy absorbed during fracture for a bcc metal can be sensitive to temperature at a strain rate

**Methodology and Specimen Preparation-Charpy Test**

Standardized tests like Charpy Testing and Izod Testing are amongst the most common types of impact tests. Charpy test is an impact test which relies on a pendulum axe that swings and collides with a Grade 23a test coupon. The geometry of the test coupons provided at University of Manchester for impact testing is of set dimensions based on American National Standards Institute (ANSI) (Zou et al, 1999). Figure 2 depicts the dimensions of the used specimen with a machined notch in the centre. The notch is where the axe strikes the specimen. This notch ensures that the stress concentration is high while maintaining high strain rate and increases the sensitivity and reproducibility of the measurements.

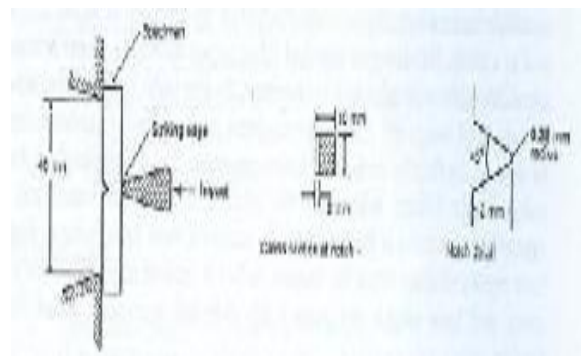


**Figure 2:** Specimen and loading configuration for Charpy V-notched impact test (Zou et. al., 1999).

It is seen that in most of the cases, the pendulum axe breaks the test coupon, depending on the material, and follows through. The degree of how far the pendulum axe follows through gives a measurement of the energy absorbed by the material during fracture. In the various tests carried out at varied temperatures, the test coupon was first immersed in a bath of liquid nitrogen and held for a few seconds so as to bring it to a low temperature of around  $-196^{\circ}\text{C}$ . Having done that, the material was then allowed to absorb surrounding heat and the temperature simultaneously measured using a temperature probe. Once the desired temperature was achieved, the test was carried out by placing the specimen on test rig and breaking it with the swing of the pendulum, as shown in Figure 3.

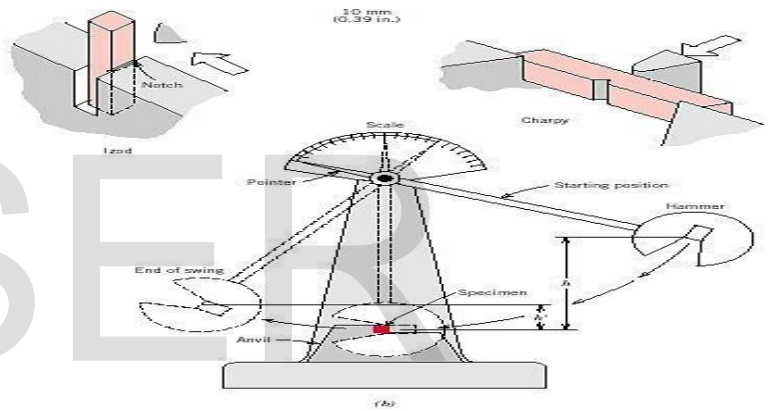


**Figure 3:** Apparatus for Charpy Impact Testing of Materials (Callister, 2009).

The panel indicated that the energy absorbed by the specimen and was measured in feet-lbs. To bring the test coupons to temperatures that are above room temperature, the coupons are immersed in a bath of hot water obtained by heating water in a kettle.

## Results of Charpy Test and Discussion

Table 1 tabulates the ten measurements at different temperatures with intervals of around 10-20 °C that were obtained to plot an energy vs. temperature graph (as shown in Figure 4) and calculate the ductile and brittle transition temperature of Grade 23a structural steel.

**Table 1:** Energy absorbed by specimen due to pendulum hammer striking the notch at different temperatures

Temperature (°C)	Energy (Feet-lb.)	Energy (J)
-71	6.5	8.8127
-39.6	6.3	8.5415
-18.2	14	18.9812
-2.6	12	16.2694
10.2	19	25.7602
20.8	51	69.1458
25	25	33.8950
31.8	166.5	225.7407
50.1	162	219.6396
69.2	168	227.7744

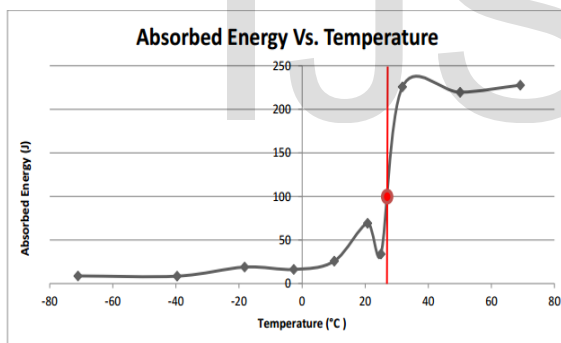


**Figure 4:** Absorbed Energy vs. Temperature Graph based on results in Table 1

According to Tanguy (2005), the DBTT Temperature can be determined by taking the centre value of the transition spikes, giving  $(31.8+25)/2 = 28.4^{\circ}\text{C}$ . In Figure 4, the red dot and proof line indicate the temperature at which a sharp decrease in impact energy occurs. We can't determine the DBTT with confidence due to the presence of certain uncertainties and random errors. Like some sources of error could be improper calibration of apparatus, cracks or irregularities on the coupon surfaces etc. Also, the estimation that the DBTT of Grade 23a steel is  $28.4^{\circ}\text{C}$  is based on assumptions like all specimens used are identical in terms of dimensions, temperature of specimen before and at the impact of the pendulum axe is the same etc. Accuracy of the Charpy test could have been improved by taking

multiple values/readings at each temperature value in order to minimize forced errors. The experiment reiterates the importance of finding the DBTT of a given material. We observe that the absorbed energy is lower below the DBTT as seen in Figure 4. At extremely low cryogenic temperatures, for instance, Grade 23a steel would be brittle instead of tough because the stresses required in steels to move dislocations in its bcc lattice are temperature dependant. If the temperature drops below  $28.4^{\circ}\text{C}$ , it would result in toughness reduction.

## EXPERIMENTAL WORK– HEAT TREATMENT OF STEEL

### Tensile Testing Material

In this part of the laboratory experiment, research was conducted on 080M46 Steel, which is equivalent to BS970 (UK) or AISI1045 steel (US) (Callister, 2009). Figure 5 depicts a 080M46 carbon steel laboratory specimen used at The University of Manchester. 080M46 Carbon steel, unlike the previous structural steel specimen, has both austenitic and martensitic properties as we would establish in due course. Carbon steels differ from structural steels with carbon content close to 0.45 wt. %. The aim was to carry out tensile tests on steel coupons with four different heat treatment conditions, i.e. before testing the coupons to coupons for their tensile strength; they were either annealed, oil quenched, water quenched or not heat treated at all. The as-received condition did not require heat treatment and was subjected to tensile testing in the condition as received from the supplier.

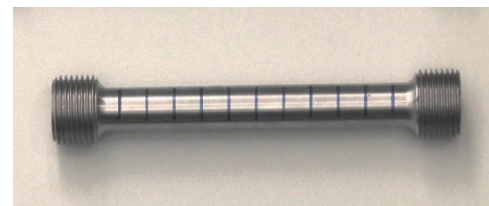


**Figure 5:** 080M46 Carbon Steel rod used for Laboratory Tensile Testing (Francis, 2014)

### Heat Treatment of Steels – Research Background

Heat Treatment of steels conveys vital information about the steel's crystal structure that, when placed on a CCT diagram, determines the different phases present in the steel sample (Reed-Hill et. al., 2009).

080M46 Steels display a wide range of mechanical properties due to iron's bcc structure at ambient temperature changing to fcc with rising temperature (Ritchie, 1976). These changes in crystal structure are significant because they directly affect the properties of steel and also because bcc and fcc crystal

structures have different solubility for carbon. The solubility property can theoretically be proven by plotting a Fe-Fe<sub>3</sub>C phase diagram as shown in Figure 6, where the thermodynamic equilibrium temperature is 723<sup>0</sup>C.

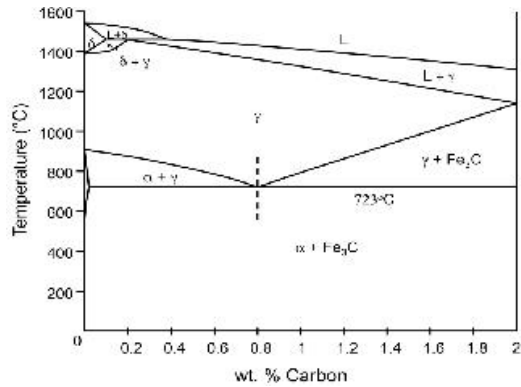


**Figure 6:** Fe-Fe<sub>3</sub>C Phase Diagram showing a low Carbon end; (Pollack, 1988)

The solubility limit for carbon in bcc iron (called ferrite – α) is approximately 0.02 wt. % and fcc iron (called austenite – γ) is 2 wt. % carbon in solid solution. If iron is cooled slowly from temperatures at which austenite is stable, to room temperature, there would be a change in its crystal structure from fcc to bcc; a thermodynamic driving force being expelled in some way due to low carbon solubility of the bcc lattice (0.02 wt. %). With slow diffusion, we also get cementite formation as second phase. With dislocations moving difficultly within cementite, the phase offers hardness and strength. Alternatively, if steel is cooled slowly from a higher temperature, a eutectoid reaction takes place due to austenite decomposition and forms a combination of austenite and cementite, called pearlite (Pollack, 1988).

However, the phase diagrams only convey the results of slow cooling of steels that allows transformations close to equilibrium. The phenomenon of water quenching involves cooling the steel rapidly and allowing no time for diffusion to take place. Under these circumstances, the driving force for the austenite to transform ferrite is strong enough to form martensite, which has a crystal structure like that of a distorted bcc lattice (Choi et. al., 1997). Martensite displays ductility and hardness due to increased carbon content. Austenite can also transform into a bcc crystal structure called bainite if it cools rapidly enough only to prevent any transformation involving substitutional diffusion but does not prevent interstitial diffusion (Bhadeshia et. al., 1980). Such microstructures of steels at room temperature can

often be inferred by comparing the cooling rate with a CCT diagram for steel. Figure 7 shows the CCT diagram obtained for 080M46 carbon steel.

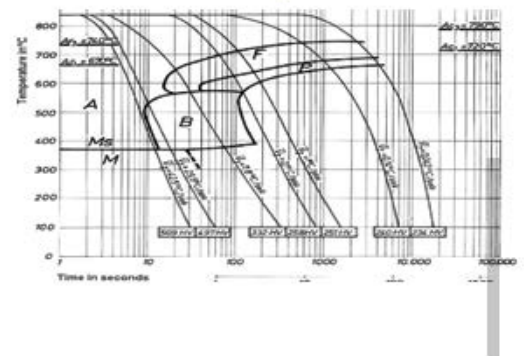


**Figure 7:** Continuous Cooling Transformation (CCT) Diagram for 080M46 Steel (Francis, 2014).

CCT diagrams are important as they show the expected start temperatures for the transformation of austenite to different phases as a function of cooling rate. ‘F’ corresponds to ferrite formation start and finish. Similarly, ‘P’ denotes Pearlite, ‘B’ denotes Bainite and ‘Ms’ denotes the start temperature for a transformation of martensite.

**Methodology and Specimen Preparation – Heat Treatment**

Transformed steel would often be strong and have high hardness, but could also be brittle. To avoid the sudden failure of steels, reduce brittleness and retain the strength, steels often undergo simultaneous heat treatment mechanisms of quenching and tempering (Q&T). This procedure involves heating the 080M46 specimens to 870°C to make it austenised, followed by its slow cooling or quenching. Slow cooling forms annealed steel and quenching forms martensite or bainite microstructures depending upon the quenching method used. The experiment requires for one specimen to be tested in as-received condition. Two test coupons are left in furnace to reach 870°C and austenisation to take place. Once heated after about 15 minutes, one coupon is transferred from the furnace to an oil bath. The other specimen is heated for an extra 5 minutes to recover heat losses due to the opening of furnace to take out the first rod. The second specimen, once heated, is transferred to fresh water bath using tongs. The slow cooling is carried out by switching off the furnace once the test coupon reaches 870°C. We let the third specimen cool inside the furnace. After drying and cleaning with tissue

	Elongation (mm)	UTS (MPa)	Yield/Proof stress (MPa)	Load at Max. Load (kN)
Annealed	24.006	423.750	298.4155	21.300
As-received	6.919	700.878	557.0423	35.230
Oil quenched	11.72	585.889	358.0986	29.450
Water quenched	6.501	1288.757	1094.1902	64.780

paper, the coupons are now ready to be tensile tested to generate a force vs. displacement plot for the four specimens. This will be useful in determining the proof/yield stress, elongation and UTS. Figure 8 shows the set up of the tensile testing device onto which the specimens, one after the other, were tested to fracture.

Figure 8: High Temperature Tensile Testing Device (Outinen, 2007)

### Results of Tensile Testing and Discussion

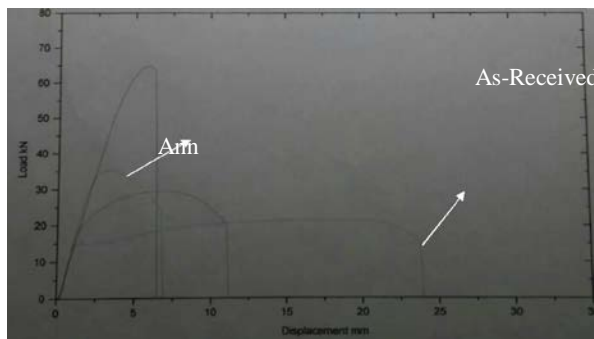


Figure 9: Load vs. Displacement Graphs after Tensile Tests of all heat treated specimen.

Figure 9 shows the computerized results obtained after the each specimen was tested to failure. These results were used to tabulate the required UTS, Yield

Stress and elongation in Table 2 with the aid of empirical formulae available.

Table 2: Results after Tensile Testing of Three heat-treated 080M46 steel specimens

The yield stress for the annealed and oil quenched steels were calculated from the graph by selecting the value of load which corresponds to the yield point and dividing it by the cross-section area to get the yield stress ( $\text{Stress} = \text{Force} / \text{Area}$ ). The proof stress for the As-received and water quenched steels are obtained by constructing a line parallel to the elastic region of the curve which offsets the line by 0.2% of the gauge length which is 100mm, hence the offset line will have its origin at 0.2mm displacement on the load vs. displacement graph. Proof load is the point at which the constructed line intersects the curve. Subsequently, the proof stress can be calculated by dividing it by the cross-sectional area.

The results obtained in Figure 7 and Figure 8 can be used to draw conclusions regarding the different phases in 080M46 steel after their heat treatment process. Water quenching process is known to have the fastest cooling rate. The conclusions we can draw from the CCT Diagram is that the water quenched specimen is expected to have predominantly austenite phase with martensitic regions dispersed in austenitic matrix. On the other hand, the Oil quenching process has a cooling rate slower than the water quenching process. The oil quenched specimen is expected to have bainite and martensite.

Looking at the results, the water quenched specimen has higher strength as compared to the oil quenched due to the presence of greater martensitic microstructures levels, thus, resulting in brittleness. On the other hand, higher toughness was seen in the water quenched specimen from the test results. However, in actual terms, the oil-quenched specimen must be having a higher toughness due to the lower levels of martensitic microstructures as compared to the water-quenched specimen. Moreover, signs of ductility were also seen beyond the yield point in the water quenched specimen but in actual terms, the material is expected to fracture either at or soon after the yield point. However, increased ductility could also have been results of higher levels of untransformed austenite present in the microstructure and thus, the degree of shear transformation that occurred during quenching might have been lesser than usual. The stress strain plot of the annealed specimen is similar to theoretical expectations. Due to the presence of martensitic microstructures in the



oil quenched specimen, it has a higher strength and lower toughness as compared to the annealed specimen. In contrast, annealed specimen has highest toughness and lowest hardness as all the effects of work hardening have been reversed. Oil-quenching results in a hard and brittle material whereas annealing reverses the effect of any hardening processes and results in a ductile and tough material.

## CONCLUSION

The laboratory experiments successfully provided the mechanical properties of the given specimen of steels, with regards to toughness and strength, under varied conditions. The Charpy Impact Test displayed that the toughness of Grade 23a steel changes with temperature. The DBTT of Grade 23a steel was found to be 28.4 °C. DBTT indicates the more suitable working conditions for given steel. We observe that the absorbed energy is lower below the DBTT as seen in Figure 4. At extremely low cryogenic temperatures, for instance, Grade 23a steel would be brittle instead of tough because the stresses required in steels to move dislocations in its bcc lattice are temperature dependant. If the temperature drops below 28.4 °C, it would result in toughness reduction. Steel Heat Treatment is performed in order to achieve the desired phases in a particular steel type which can be monitored using a CCT diagram. We know that quenching and tempering mechanisms increase hardness, strength and toughness of a given material. The experiment was crucial in establishing that strength and toughness of 080M46 steel vary depending on heat treatment and Q&T technique at approximately 870°C.

## ACKNOWLEDGEMENTS

The author would like to thank fully appreciate the help and support received from The University of Manchester's Materials Laboratory and Material Science staff for their fruitful guidance.

## REFERENCES

1. Baddoo, N.R. (2008). Stainless Steel in Construction: A review of research, applications challenges and opportunities. *Journal of Constructional Steel Research*. 64(11). [Online].
2. Bhadeshia, H.K.D.H and Edmonds, D.V. (1980). The mechanism of bainite formation in steels. *Acta Metallurgica*. 28(9)
3. Callister, W.D. (2009). *Materials Science and Engineering - An Introduction – Edition 6*. John Wiley & Sons.
4. Choi, J.Y. (1997). Strain induced martensitic formation and its effect on strain hardening behavior in the cold drawn 304 austenitic stainless steel. *Scripta Materialia*. 36(1). [Online].
5. Francis, J. (2014). *Stainless Steels. MACE20037Materials 2*. University of Manchester. (Unpublished).
6. Gavriljuk, V.G., Teus, S.M, Shivanyuk, V.N and Shanina, B.D. (2007). Effects of hydrogen and electronic structure of fcc iron in relation to hydrogen embrittlement of austenitic steels. *Applications and Material Science*. 204(12).
7. Khaleghi, M and Haynes, R. (1985). Sintering and Heat Treatment of Steels Made from a Partially Prealloyed Iron Powder. *Maney Online*. 28(4). Pp 217 – 223.
8. Outinen, J. (2007). *Mechanical Properties of Structural Steels at High Temperature and After Cooling Down*. Doctoral Dissertation. Helsinki University of Technology.
9. Lo, K.H., Shek, C.H. and Lai, J.K.L. (2009). Recent Developments in Stainless Steels. *Material Science and Engineering Reports*. 65(4). Pp 39 – 104.
10. Pandiyan, T., Roque, J.M., Cruz, J. and Garcia-Ochoa, E. (2008). DFT and electrochemical studies of tris(benzimidazole-2-ylmethyl)amine as an efficient corrosion inhibitor for carbon steel surface. *Corrosion Science*. 50(3)
11. Pollack, H.W. (1988). *Materials Science and Metallurgy – 4<sup>th</sup> Edition*. Prentice-Hall, Englewood Cliffs, NJ.
12. Ritchie, R.O., Francis, B. and Server, W.L. (1976). Evaluation of toughness in AISI 4340 alloy steel austenitized at low and high temperatures. *Mechanical Behavior*. 7(6). [online]. Accessed through Springer Link database. [Accessed on November 19<sup>th</sup>, 2015].
13. Tanguy, B. Besson, J. Piques, R and Pineau, A. (2005). Ductile to Brittle Transition of an A508 steel characterized by Charpy Impact Test: Part 1: Experimental Results. *Engineering Fracture Mechanics*. 72(1). [Online]. Accessed through Science Direct database. [Accessed on November 17<sup>th</sup>, 2015].
14. Zhou, M., Hu, S., & Zhang, H. (1999). Critical specimen sizes for tensile-shear testing of steel sheets. *Welding Journal*.

IJSER

IJSER